MINISTRY OF EDUCATION AND TRAINING

VIETNAM ACADEMY OF SCIENCE AND TECHNOLOGY

GRADUATE UNIVERSITY SCIENCE AND TECHNOLOGY

PHAM THANH BINH

RESEARCH AND FABRICATION OF OPTO-CHEMICAL SENSORS BASED ON OPTICAL FIBER FOR APPLIED TO DETECT SOME HAZARDOUS CHEMICALS IN THE ENVIRONMENT

Major: Optical Materials, Optoelectronics and Photonics

Code: 9. 44. 01. 27

SUMMARY OF MATERIAL SCIENCE DOCTORAL THESIS

HANOI - 2023

PhD Thesis was completed at Graduate University of Science and Technology, Vietnam Academy of Science and Technology.

Supervisors:

1. Assocc. Prof. Dr. Pham Van Hoi
2. Assocc. Prof. Dr. Bui Huy

Reviewer 1: Prof. Dr. Chu Manh Hoang

Reviewer 2: Assocc. Prof. Dr. Tran Quang Huy

Reviewer 3: Assocc. Prof. Dr. Nguyen Thanh Tung

The dissertation will be defended at Graduate University of Science and Technology, 18 Hoang Quoc Viet street, Hanoi.

The thesis could be found at:

- National Library of Vietnam
- Library of Graduate University of Science and Technology
- Library of Institute of Science Materials

INTRODUCTION

1. The urgency of the thesis

Nowadays, the life environment (including food, air, water, pharmaceuticals and pre-pharmaceuticals...) has been seriously polluted. Therefore, the good monitoring of environmental pollutants is an urgent issue in the human society of countries and Vietnam. The research and development of technologies for manufacturing sensing components and devices to detect and control toxic agents in the life environment is great interested in the research and technology deployment facilities in the world. Sensors suitable for the control of contaminated life environment have strict requirements such as: non-rust, long operating time and high repeat of measurement results, low detection limit of measured substances (ppm or lower) and has good selectivity for each pollutant. Traditional analysis methods such as gas chromatography, and liquid chromatography and mass spectrometry have demonstrated the ability to detect and measure concentrations of bio-chemical contaminants with very small amounts (possibly up to the molecular level), however, these analysis methods are very expensive because the equipment is expensive and the sample making process is quite complicated, the analyst needs a very careful and long time of professional training, so it is difficult. disseminate these techniques on a large range. Therefore, the research, manufacture and development of low-cost, compact, easy-to-use and highly sensitive in different environments sensing devices to recognize, detect, monitor and control the physico-chemical parameters and the degree of contamination of biological and chemical substances in the life environment, especially in food are

highly topical. One of the new generation sensors is being developed very much that is photonic sensors because they have many unique advantages. Photonic sensing devices have emerged as a very strong research and development object to detect and quantitatively measure harmful agents in the environment because of its many outstanding properties. Photonic sensing devices have been studied and applied in the field of controlling harmful agents in the environment with many different types. In which, optical fiber-based photonic sensors have been very interested and developed in the world because of many outstanding advantages such as being able to be used for in-situ measurements, immunity from interference of electromagnetic fields, very stable operating in chemistry etching environments or in conditions of high temperature and pressure, and not generate sparks in environments, no risk of fire or short circuit due to be not required power supply the probe. Optical fiber sensor with sensing element to be a part of the optical fiber itself is developed based on the principle of light transmission in optical fiber that interact with the external environment to change the intensity, frequency (wavelength), polarization and direction propagation of lights... Moreover, the stability of optical fiber sensor in the natural environment is very high (no rust due to oxidation, and especially safe in the environment) because the optical fiber sensor is faricated by silica glass. With the very strong development of optoelectronic and photonic materials and components in recent times, optical fiber sensors are easy and convenient to integrate with excitation light sources by diode laser, optical receiver by photodiode semiconductor, and high resolution photoelectric signal processor and analyzer [1-9]. Recently, there have been many scientific and technological studys of

many research groups in the world publish of the field of research and development of optical fiber sensors such as bio-chemical sensors designed with probe structure to be singlemode-multimode-singlemode optical fiber (SMS) [10], optical fiber sensor using fiber Bragg grating (FBG) [11-13], optical sensor with optical fiber probes based on surface plasmonic resonance enhancement effect and surface enhancement Raman scattering (SERS) effect [14,15]. Each type of sensor mentioned above has its own advantages and limitations, however, configurations of optical fiber sensors have many outstanding advantages compared to other types of sensors such as very high sensitivity, simple structure, compact and oriented to integrate with portable equipment good operating in the fact, and friendly to the environment, and especially easy to integrate with terminals, and transmit signals over long distances based on optical fiber communication system. On the basis of analyzing the practicality and urgency in the research direction of opto-chemical sensors based on optical fiber, I select for the research topic of my doctoral thesis with the research content in the field of Optical Materials, optoelectronics and photonics with the title as: "***Research and fabrication of opto-chemical sensors based on optical fiber for applied to detect some hazardous chemicals in the environment".***

2. The objectives of the thesis

i) Fabrication of a opto-chemical sensor based on FBG components to be integrated in fiber lasers to develop into a high-sensitivity sensor device that ensures standards in the analysis of toxic contaminants in the aquatic environment.

ii) Fabrication of optical sensors based on surface plasmonic resonance effect, and surface enhanced Raman scattering effect on

optical fibers with Au/Ag noble metals nanoparticles directly synthesized onto fiber surface by laser assisted photochemical method with wavelengths (between 532nm and 980nm) and application in detecting residues of pesticides in the environment accordance with food safety standards.

3. The main contents of the thesis

i) Research and fabrication of opto-chemical optical fiber sensor based on FBG integrated into a loop-mirror optical fiber laser.

ii) Application of analysis of Nitrate and some organic solvents with variable refractive index in the range of 1.42 RIU-1.44 RIU.

iii) Research and fabrication of opto-chemical optical fiber sensor based on surface enhancement Raman scattering effect on optical fiber substrates with gold/silver nanostructures.

iv) Application of analysis of some pesticides (Permethrin, dimethoate, fenthion, cypermethrin).

Thesis structure:

The thesis is built with an introduction that presents the meaning and reasons for choosing the research issues and the general conclusion state the main results that have been achieved as well as some issues that can be further studied in the thesis. The part of the thesis main content is divided into five chapters. In which, the first two chapters present the theoretical basis and overview of optical fiber sensors. Especially, the opto-chemical optical fiber sensor based on FBGs, and SERS optical fiber subtrates. The last three chapters are experimental results of fabrication, surveying the characteristics of two types of sensors and testing two types of sensors prepared to analyze some chemicals and pesticides those are toxic to the

environment. At the end of the thesis, a list of publications are used in the thesis and related publications.

CHAPTER 1:

OVERVIEW ABOUT OPTICAL FIBER SENSOR

In this chapter, we first introduce in the structure and the operating principle of optical fiber. Next, the concept, outstanding advantages and applicability of optical fiber sensors in general and especially optical fiber sensors based on evanescent field wave technique are presented.

CHAPTER 2:

THEORY OF OPTO-CHEMICAL OPTICAL FIBER SENSING BASED ON FBG AND PLASMON RESONANCE EFFECT

The first part of the chapter presents the optical fiber Bragg grating (FBG) - an optical fiber segment with cyclic variation of the refractive index in the core of a single-mode optical fiber, the operating principle of the FBG as well as the possibility of using it in the field of sensors. Next, we present the concept of the plasmon effect and its application in the field of opto-chemical optical fiber sensing. The localized surface plasmon resonance effect applied in opto-chemical sensor based on surface enhancement Raman scattering effect is also mentioned. The last part of the chapter is devoted to the evaluation of the high-performance SERS optical fiber substrates.

CHAPTER 3:

FABRICATION OF OPTO-CHEMICAL OPTICAL FIBER SENSOR AND SENSING DEVELOPMENT BY INTEGRATED D-FBG INTO A LOOP - MIRROR OPTICAL FIBER LASER

3.1. Fabrication of opto-chemical optical fiber sensor based on FBG

The opto-chemical optical fiber sensor based on FBG is operated via the variation of the refractive index. Figure 3.1 illustrates the structure of the prepared FBG sensor by chemical etching method (e-FBG), and by mechanical side-polished method (D-FBG). [161, 162].

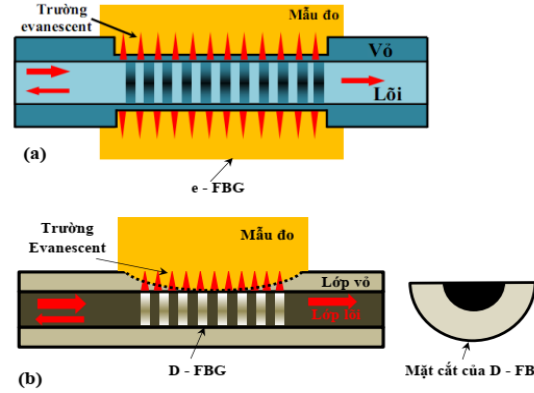

Figure 3.1. The structure of the optical fiber sensor (a) e – FBG and (b) D-FBG.

3.1.1. Chemical etching method

The process of the fabricated opto-chemical FBG sensing element by chemical etching method (e-FBG: etched-FBG) has been designed with a schematic diagram of the experimental setup shown in Figure 3.2.

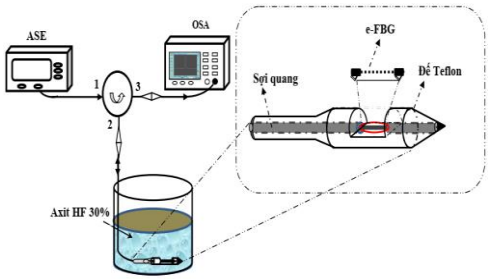

Figure 3.2. schematic diagram of the fabricated opto-chemical FBG sensing element by chemical etching method experimental setup.

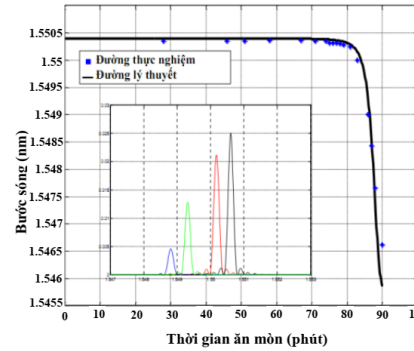

Figure 3.3. The characteristic curve of the reflected wavelength shift of the e-FBG versus the etching time

3.1.2. Surveying the characteristics of the e-FBG sensor

Figure 3.3 shows the reflected wavelength shift characteristic curve of the e-FBG sensor changing with the etching time in HF solution of 30% concentration performed with a period of 90 minutes and recorded from The experimental (dotted line) along with the theoretical line (solid line) according to the mathematical model have been presented in the theoretical part.

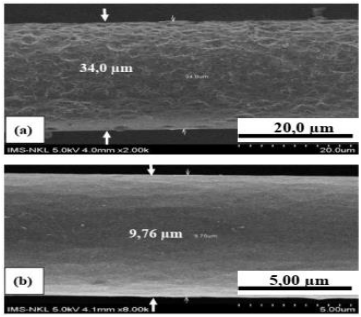

Figure 3.4. SEM images of the e - FBG sensor after coarse etching (a), and fine etching (b).

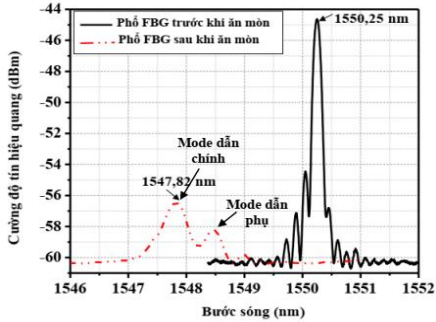

Figure 3.5. Reflected spectra of the FBG sensor before and after etching process.

In figure 3.4 (a), SEM image of the e - FBG sensor after rough etching, it is shown that the diameter of the optical fiber in the FBG region decreased significantly from 125 µm to 34 µm and the surface appeared many pores with the large roughness of surface due to the rapid corrosion process. The SEM image of the e-FBG after fine etching process is presented in Figure 3.4(b). The SEM image results also show that the diameter of the optical fiber in the etched FBG region is reduced to 9,76 µm which almost completely removes the crust and the smooth surface almost eliminates the porosities due to the corrosion rate in this process is very slow. The transformation of the e-FBG reflected spectral signal is presented in Figure 3.5. In

which, the peak of the reflected spectrum of e-FBG is shifted by 2.43 nm and the full width at half-maximum spectral at 3 dB is also extended by 0.52 nm compared to the reflectance spectrum of the original FBG. Beside, we also notice a significant reduction in the reflected signal strength from -45.4 dBm to -57.6 dBm and enabling it to induce adjacent modes that can be shell modes.

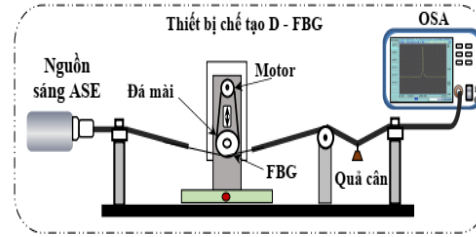

Figure 3.6. Schematic diagram of D shaped-FBG polishing

3.1.3. The mechanical side-polished method

The fabricating process of D-FBG sensor by mechanical side-polished method has the directly control of the transmission spectrum signal of FBG via the optical spectrum analyzer OSA. The schematic diagram of the device system of fabricating D-FBG probes by mechanical side-polished method is illustrated in Figure 3.6.

3.1.4. Surveying the characteristics of the D-FBG sensor

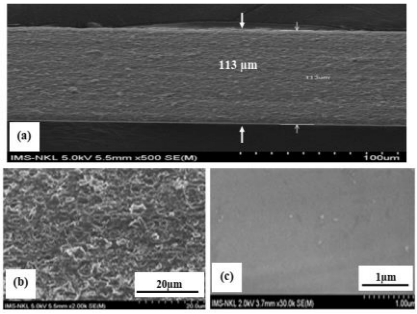

Figure 3.7. SEM images of D-FBG sensor after side-polishing.

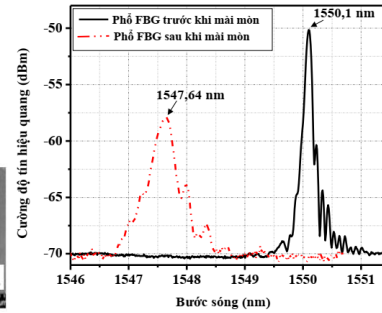

Figure 3.8. Reflected spectra of the D-FBG sensor before and after side-polishing

Figure 3.7 (a, b) depict the SEM images of the D-FBG sensor after rough polishing, we can observe that the polishing area with a width

of up to 113 µm and a relatively large surface roughness due to the fast wear rate. After performing the fine polishing process, the surface of the D-FBG sensor area is also surveyed via SEM images with large magnification of 30,000 times and shown in figure 3.7 (c). The SEM image results after the fine polishing process, indicate that the surface of the D - FBG sensor area has been smoothed and almost eliminated the porous layers and large scratches because of the use of a grinding stone with small particles size in this process, thus reducing light scattering caused on the fiber surface. Figure 3.8 clearly shows that the peak of the reflected spectrum of D-FBG is shifted by 2.46 nm and the full width at half-maximum spectrum at 3 dB is also expanded by 0.46 nm compared to the reflectance spectrum of the original FBG of 0.2 nm. Beside, we also noticed a reduction in the reflected signal strength of 8.2 dB.

3.2. Development of a opto-chemical optical fiber sensor based on the D-FBG integrated in a loop-mirror fiber laser

3.2.1. The structure of the sensor

The structure of the opto-chemical sensor with D - FBG integrated in the fiber laser is built with the configuration presented in Figure 3.9.

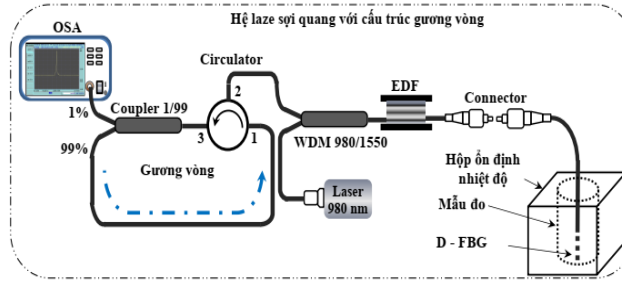

Figure 3.9. Schematic diagram of opto-chemical sensor based on D-FBG integrated in the fiber laser with the loop-mirror structure

3.2.2. The operating principle of the sensor

The D-FBG sensing probe operates based on the interaction between the fundamental light mode in the optical fiber and the surrounding environment at the sensing region, and the refractive index changes of the surrounding medium corresponding to the Bragg wavelength displacement.

3.2.3. Surveying the characteristics of opto-chemical sensors based on D-FBG integrated in a fiber laser with loop-mirror structure

The measurement results presented in figure 3.10 shows and directly compare the characteristics spectral signal of the D-FBG sensor with the reflectometer configuration (solid lines) and the proposed fiber laser measurement configuration (dashed lines) to demonstrate that with the proposed fiber laser measurement configuration significant improvement in spectral characteristics..

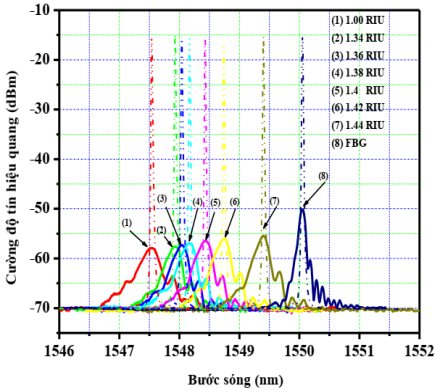

Figure 3.10. The spectra signal of the opto-chemical sensor based on D-FBG with the reflectometer configuration (solid lines) and the proposed fiber laser measurement configuration (dashed lines) are performed in the liquid medium of the refractive index changes in range of 1 RIU - 1.44 RIU.

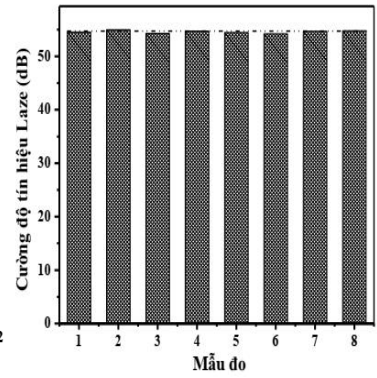

Figure 3.11. The optical signal intensity of the D - FBG sensor with the fiber laser measurement configuration in liquid medium with variable refractive index in the range of 1.00 RIU – 1.44 RIU.

The measured results presented in Figure 3.11 shows that the spectral signal intensity of the D - FBG sensor integrated in a fiber laser configuration with loop-mirror structure and used saturation pumping technique is very huge about 55 dB and very stable in liquid media with variable refractive index in the range of 1.00 RIU-1.44 RIU corresponding to measured samples from 1 to 8.

CHAPTER 4:
FABRICATION AND SURVEY OF THE CHARACTERISTICS OF SERS OPTICAL FIBER SUBSTRATE WITH GOLDEN/SILVER NANOSTRUCTURES BY SEMICONDUCTOR LASER ASSISTED PHOTOCHEMICAL METHOD

4.1. Fabrication of SERS substrates on the end of optical fiber with Ag nanostructures

The fabricating process of the flat optical fiber SERS substrates with silver nanostructures directly synthesized by photochemical method using laser light source emitted at wavelegnth of 532 nm is detailed shown in Figure 4.1.

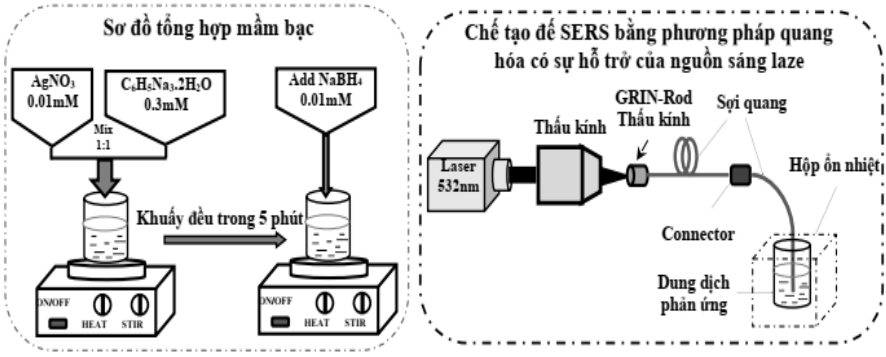

Figure 4.1. The fabricating schematic diagram of the flat optical fiber SERS substrates with silver nanostructures.

The flat optical fiber SERS substrates with Ag nanostructures synthesized by laser illumination according to the exposure time, and used for measurement of Raman spectroscopy of R6G reagent (10^{-5} M), as shown in Figure 4.7.

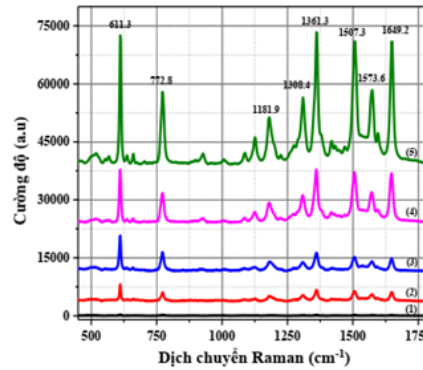

Figure 4.7. SERS spectra of R6G solution (10^{-5} M) on those flat optical fiber SERS substrates with Ag nanostructures synthesized by laser illumination according to the exposure time.

The obtained Raman spectra results show that the Raman enhancement effect of the flat optical fiber SERS substrates with different silver nanostructures is markedly different. The obtained characteristic Raman signal intensity of R6G adsorbed on a flat optical fiber SERS substrate with AgNDs nanostructure is the highest. The EF calculation results are performed, and these results are presented in Table 4.2.

Table 4.2. Values of the enhancement factor of characteristic Raman signals of R6G-adsorbed on the flat optical fiber SERS substrates with different silver nanostructures.

Laser exposure time (minutes)	**Raman shift (cm^{-1})**							
	611,3	**772,8**	**1181,9**	**1308,4**	**1361,3**	**1507,3**	**1573,6**	**1649,2**
2 (2)	$1,42x10^6$	$1,02x10^6$	$9,75x10^6$	$9,61x10^5$	$1,22x10^6$	$1,05x10^6$	$1,02x10^6$	$1,45x10^6$
5 (3)	$2,97x10^6$	$2,16x10^6$	$1,8x10^6$	$1,37x10^6$	$1,98x10^6$	$1,44x10^6$	$1,41x10^6$	$1,99x10^6$
7 (4)	$4,45x10^6$	$3,4x10^6$	$3,89x10^6$	$4,38x10^6$	$5,77x10^6$	$5,25x10^6$	$4,56x10^6$	$7,78x10^6$
9 (5)	$1,08x10^7$	$8,31x10^6$	$9,1x10^6$	$1,07x10^7$	$1,43x10^7$	$1,28x10^6$	$1,1x10^7$	$1,93x10^7$

4.2. Fabrication of microsphere optical fiber SERS substrates with Au/Ag nanostructures

The fabricating process of SERS substrate onto top of optical fiber microspheres with AuNPs/AgNDs nanostructures directly synthesized by photochemistry using two laser light sources simultaneously is presented in detail in Figure 4.11.

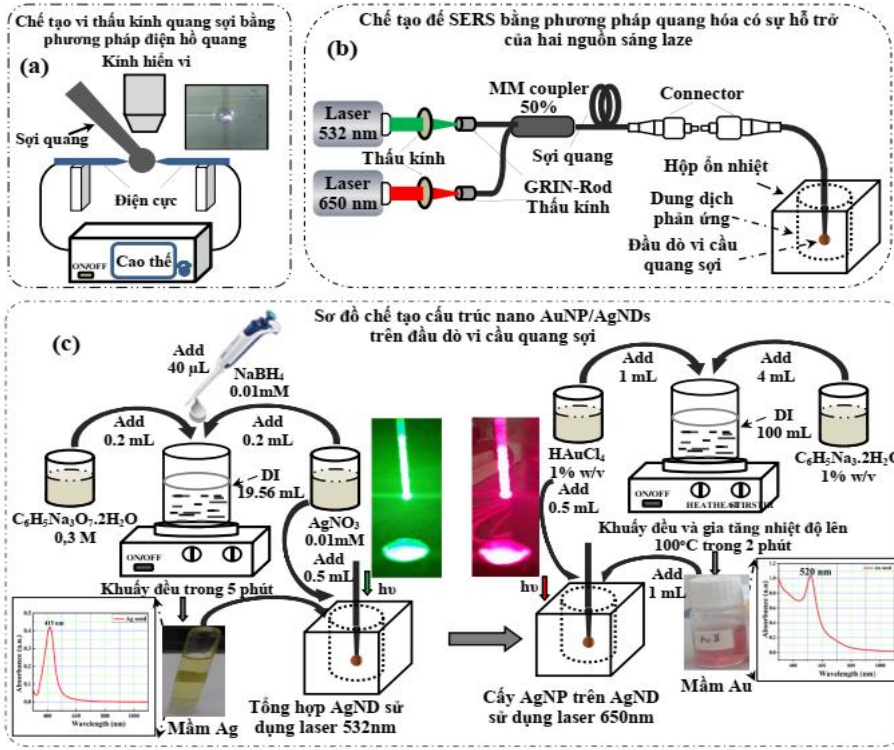

Figure 4.11. Sơ đồ quy trình chế tạo đầu dò vi cầu trên sợi quang có phủ cấu trúc nano AuNP/AgND.

Figure 4.15 (a, b and c) presents the optical images and SEM images of the microsphere optical fiber probe after synthesized the Au metal nanoparticles on the surface of the AgNDs metal nanostructure. We can easily observe the Au metal nanoparticles uniformly distributed on the surface of the AgNDs nanostructure mounted on top of the

microsphere optical fiber substrates. Besides, the information from the energy-dispersive X-ray (EDX) spectrum presented in Figure 4.15(d) has also demonstrated that on the very clean fiber probe sample, there are only characteristic peaks of Au and Ag elements, because Au and Ag metal nanoparticles synthesized and attached on the surface of the microsphere optical fiber probe and the elements Ge, Si, O are the components of the optical fiber with Ge doped into SiO2.

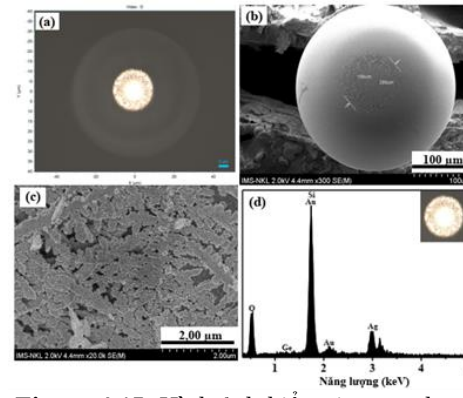

Figure 4.15. Hình ảnh hiển vi quang học và ảnh SEM của đầu dò vi cầu sợi quang sau khi được tổng hợp các hạt nano vàng lên cấu trúc cành lá bạc.

Raman spectra of the same reagent R6G solution (10^{-5} M) on different SERS substrates with different metal nanostructures on microsphere optical fiber substrates, and the Raman spectra results were recorded as shown in Figure 4.17. These Raman spectra also clearly show that the SERS enhancement effect of microsphere optical fiber SERS substrates with AgNDs nanostructures before and after AuNPs implantation is superior to that of microspheres optical fiber SERS substrates with AuNPs nanostructures. In

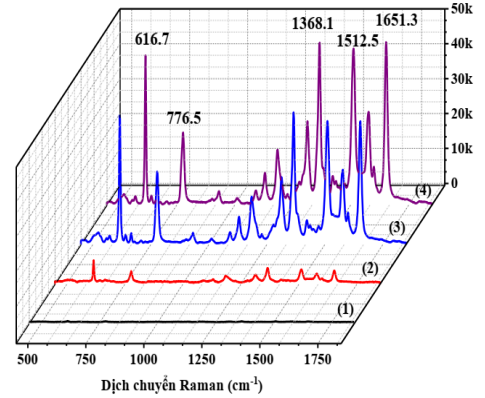

Figure 4.17. SERS spectra of R6G solution (10^{-5} M) recorded for the spheroid end-facet optical fiber SERS substrate without nanometallic deposition (curve 1), and the spheroid end-facet optical fiber SERS substrate with coated AuNPs (curve 2), AgNDs nanostructures (curve 3) and AuNPs/AgNDs nanostructures (curve 4).

particular, the obtained characteristic Raman signal intensity of R6G adsorbed from the microsphere optical fiber SERS substrate with AuNPs/AgNDs nanostructure is the highest. The EF is calculated for different types of microsphere optical fiber SERS substrates with different nanostructures, and is shown in Table 4.3.

Table 4.3. Values of Raman scattering enhancement factor of R6G solution (10^{-5} M) prepared on microsphere optical fiber SERS substrate with metal Au/Ag nanostructures.

The microsphere optical fiber SERS substrate with metal Au/Ag nanostructures	**Raman shift (cm^{-1})**	
	616,7	1368,1
AuNPs	$2,09 \times 10^6$	$2,28 \times 10^6$
AgNDs	$1,2 \times 10^7$	$2,07 \times 10^7$
AuNPs/AgNDs	$1,4 \times 10^7$	$2,54 \times 10^7$

CHAPTER 5:
APPLICATION OF OPTO-CHEMICAL SENSOR BASED ON OPTICAL FIBER FOR DETECTION OF SOME HAZARDOUS CHEMICALS IN THE ENVIRONMENT

5.1. Application of optical fiber opto-chemical sensor based on FBG for detection of nitrate and some organic solvents in liquid medium

5.1.1. Application of optical fiber opto-chemical sensor based on e-FBG integrated into a loop-mirror fiber laser for detection of nitrate in liquid medium

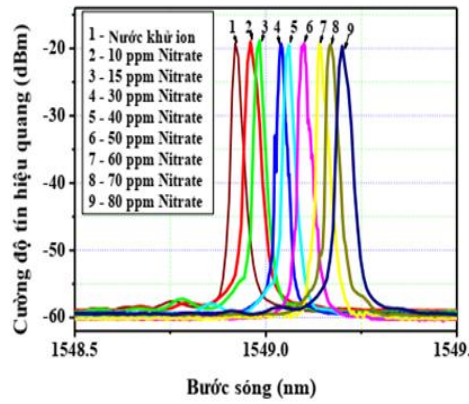

Figure 5.1. The spectra of optical signals of the e-FBG sensor as perform to measuring nitrate solutions with concentration varies from 10 ppm to 80 ppm.

The measuremental results with nitrate solution samples with changing concentrations ranging from 10 ppm to 80 ppm were recorded through the OSA instrument, and presented in Figure 5.1.

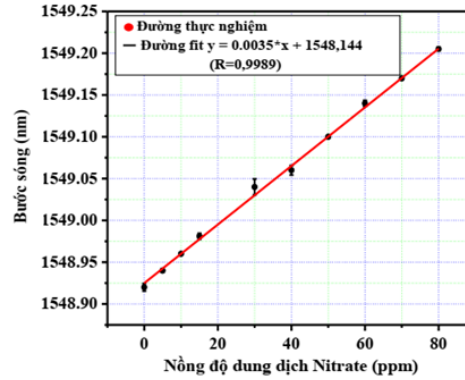

Figure 5.2. The characteristically line of the signal wavelength shift of the e-FBG sensor as the concentration of the Nitrate solution

From the results obtained in Figure 5.2, it shows that the signal wavelength of the e-FBG sensor and the concentration of nitrate solution have a linear relationship and are matched linearly with the equation y = 1548,144 + 0.0035x (nm) with R = 0.9989. The slope of the linearly characteristically line is 0.0035 nm/ppm, and the limit of detection LOD of sensor can be calculated as LOD = 3 ppm.

5.1.2. Application of optical fiber opto-chemical sensor based on D-FBG integrated into a loop-mirror fiber laser for detection of some organic solvents

From the results presented in Figure 5.3, it is shown that the sensing signal spectral to be a laser spectral, so it has a narrow spectral width of 0.01 nm and a very large signal strength of about 50 dB and relatively uniform, and also found that clearly sensing signal spectral shift to long wavelengths as perform measuring analytical samples with increased refractive index. From the experimental measurement points obtained in Figure 5.4, we perceive that the signal wavelength of the D-FBG sensor with the proposed measurement configuration and the refractive index of the analyzing sample has a relatively

linear relationship and also matched linearly with the equation: y = 15500,54 + 33,94*x (nm) with R^2 = 0,998.

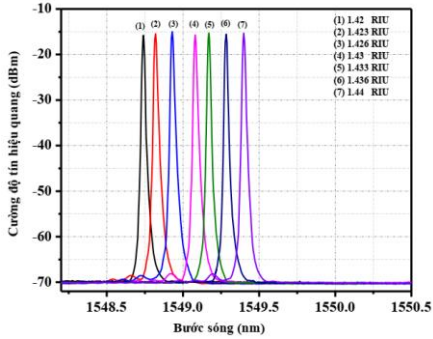

Figure 5.3. Signal spectral of the sensor as perform measuring with analytical samples with refractive index in the range of 1.42 RIU - 1.44 RIU.

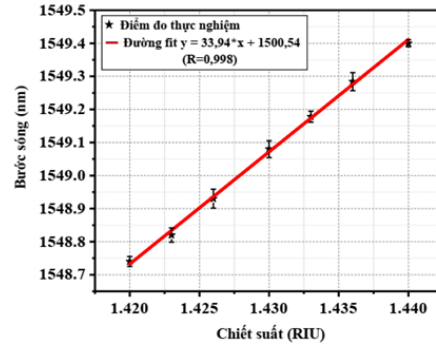

Figure 5.4. The characteristically line of the dependence between the signal wavelength shift of the D-FBG sensor and the refractive index changes in the range 1.42 – 1.44 RIU.

The slope of the linearly characteristically line of 33,94 nm / RIU can be viewed as the sensor sensitivity usually defined as S= $\partial\lambda/\partial C$, with a resolution of measuring device Res = 0,01 nm the limit of detection LOD of the sensor is determined to be 2,95 x 10^{-4} RIU.

5.2. Application of optical fiber SERS substrates with AgNDs and AuNPs/AgNDs nanostructures for detection of some pesticides.

5.2.1. Application of optical fiber SERS substrates with AgNDs nanostructures for detection of Permethrin pesticides.

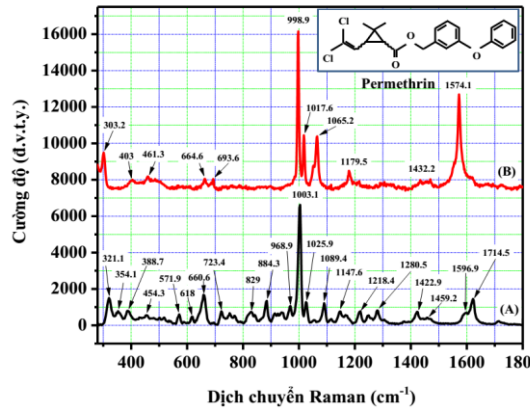

Figure 5.5. Raman spectrum of pure Permethrin on a flat optical fiber substrate (A) and Permethrin solution (10 ppm) on a flat optical fiber SERS substrate with AgNDs nanostructure (B).

The results of measuring Raman spectral of pure Permethrin on flat optical fiber substrate and a Raman spectrum of Permethrin solution with concentration of 10 ppm on a flat optical fiber SERS substrate with AgNDs nanostructure are presented in Figure 5.5, and clearly show the characteristic spectral peaks correspond to the oscillation modes. Figure 5.6 shows the Raman spectral of Permethrin solutions, and demonstrates the analytical capabilities that can be achieved with this SERS substrate for Permethrin analytes at concentrations as low as 0.1 ppm.

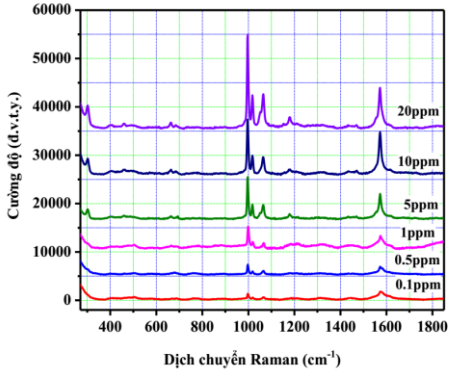

Figure 5.6. Raman spectral of Permethrin solution with concentrations of 0.1 ppm, 0.5 ppm, 1 ppm, 5 ppm, 10 ppm and 20 ppm on flat optical fiber SERS substrates with AgNDs nanostructure.

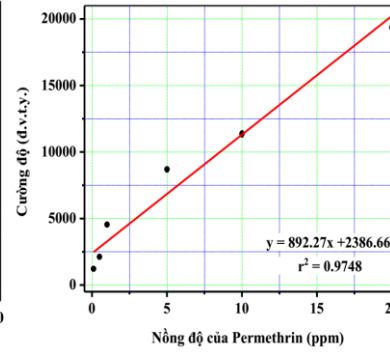

Figure 5.7. The characteristically curve of the dependence between Raman signal of Permethrin at the characteristic spectrum peak of 998.9cm^{-1} according to the concentration of Permethrin solutions.

Figure 5.7 shows a good linear relationship between the SERS signal intensities and the concentration of Permethrin solutions, with the regression equation as:y = 2386.66 + 892.27*x (đ.v.t.y) with deviation R = 0,9748, and the limit of detection of the measurement that can be calculated as LOD = 0.0035 ppm.

5.2.2. Application of microsphere optical fiber SERS substrates with AgNDs nanostructures for detection of Dimethoate pesticides.

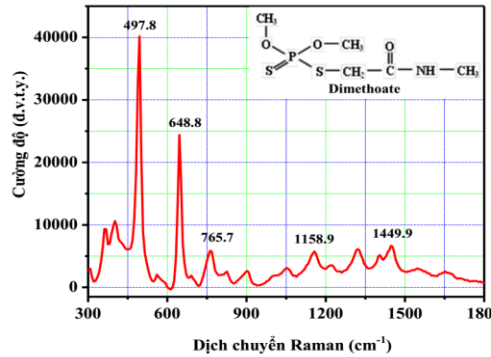

Figure 5.8. Raman spectrum of Dimethoate solution with concentration of 20 ppm on a microsphere optical fiber SERS substrate with AgNDs nanostructure.

The results of measuring Raman spectrum of Dimethoate solution with concentration of 20 ppm on the microsphere optical fiber SERS substrate with AgNDs nanostructure are presented in Figure 5.8. Raman spectrum clearly show characteristic spectral peaks corresponding to the vibrational modes of the Dimethoate molecule. Figure 5.9 presents the results of Raman spectral of Dimethoate prepared with different concentrations of 0.05 ppm (1), 0.1 ppm (2), 1 ppm (3), 2 ppm (4) and 10 ppm (5) on a microsphere optical fiber SERS substrate with AgNDs nanostructures. The results show that the Raman spectral signal intensity of Dimethoate with low concentration range is greatly enhanced and the peak separation is very clear, the signal peak is attenuated as the concentration of Dimethoate analyte decreases. From the experimental results, we have built a linearly regression line depicting the dependence between the peak intensity of the strongest characteristic SERS signal of Dimethoate at 497.8 cm-1 and the concentration of Dimethoate, and shown in Figure 5.10. The result shows a good linear relationship between the SERS signal intensities and the concentration of Dimethoate solutions, with the

regression equation as: y = 975.66 + 2667.12*x (đ.v.t.y) with deviation R = 0.992, and the limit of detection of the measurement that can be calculated as LOD = 0.001 ppm.

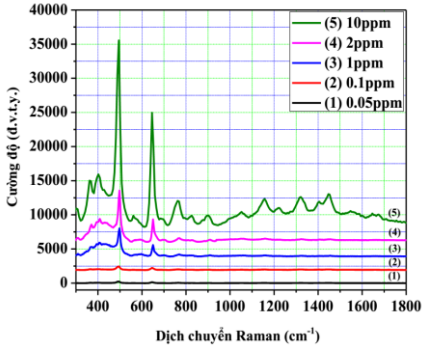

Figure 5.9. Raman spectral of Dimethoate solution with different concentrations on microsphere optical fiber SERS substrates with AgNDs nanostructure.

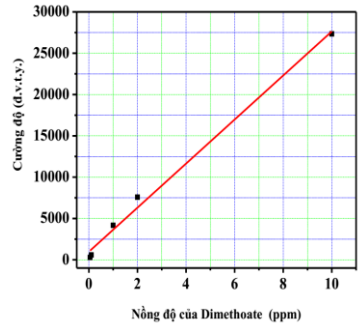

Figure 5.10. The characteristically curve of the dependence between Raman signal of Dimethoate at the characteristic spectrum peak of 497.8 cm^{-1} according to the concentration

5.2.3. Application of microsphere optical fiber SERS substrates with AuNPs/AgNDs nanostructures for detection of Fention and Cypermethrin pesticides.

Raman spectra of samples of Fenthion standard analytical solutions with concentrations of 0.005 ppm; 0.01 ppm; 0.05 ppm; 0.1 ppm; 0.2 ppm; 0.5 ppm; 1 ppm and 2 ppm are shown in Figure 5.11. SERS spectrum of Fenthion on the microsphere optical fiber SERS substrate with AuNPs/AgNDs nanostructure has complex with many spectral peaks distributed in the region of 450 cm^{-1}-1800 cm^{-1}. Figure 5.12 shows the linearly relationship between the SERS signal intensties and the concentration of Fenthion solutions, with the regression equation as: y = 7904.86*x + 336.58 (đ.v.t.y) with

deviation R = 0.995 and the limit of detection of the calculated measurement is LOD = 1.7 x 10^{-4} ppm.

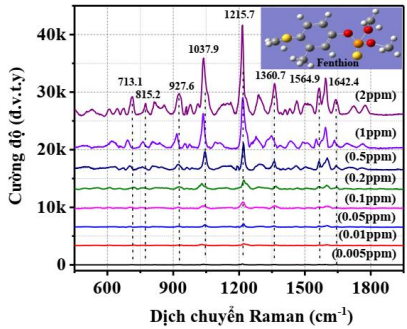

Figure 5.11. Raman spectral of Fenthion solutions with different concentrations on a microsphere optical fiber SERS substrate with AuNPs/AgNDs nanostructures.

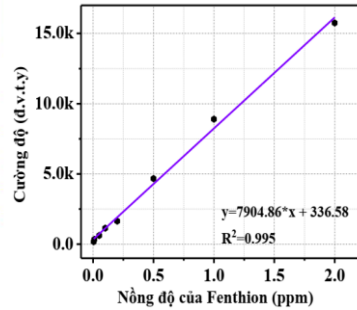

Figure 5.12. The characteristically curve of dependence between Raman signal of Fention at the characteristic spectrum peak of 1215,7 cm^{-1} and concentration.

Raman spectra of Cypermethrin standard solution samples with concentrations of 0.001 ppm; 0.005 ppm; 0.01 ppm; 0.05 ppm; 0.1 ppm; 0.5 ppm and 1ppm were prepared on microsphere optical fiber SERS substrates with AuNPs/AgNDs nanostructures, and shown in Figure 5.13.

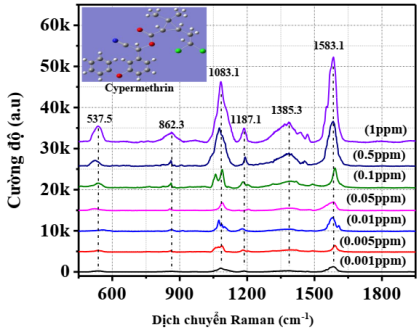

Figure 5.13. Raman spectral of Cypermethrin solutions with different concentrations on a microsphere optical fiber SERS substrate with AuNPs/AgNDs nanostructures.

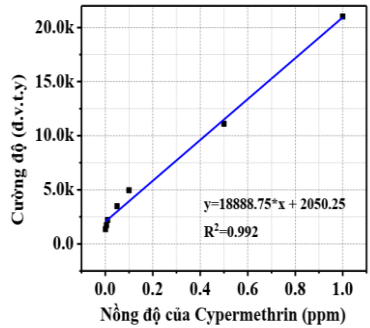

Figure 5.14. The characteristically curve of dependence between Raman signal of Cypermethrin at the characteristic spectrum peak of 1583,1 cm^{-1} and concentration.

The SERS spectrum of Cypermethrin on the microsphere optical fiber SERS substrate with AuNPs/AgNDs nanostructures has spectral peaks distributed in the region of 500 cm^{-1} - 1700 cm^{-1}. Figure 5.14 can be seen that there is a good linearly relationship between the SERS signal intensities and the concentration of Cypermethrin solutions, with the regression equation as: y = 18888,75*x + 2050,25 (a.u)) with a deviation R = 0,992 and the limit of detection of the measurement that can be calculated as LOD = 2,87 x 10^{-4} ppm.

CONCLUSION

The thesis has focused on the study and fabrication of optical fiber opto-chemical sensor based on FBG element and opto-chemical sensor based on SERS effect based on optical fiber with gold/silver nanostructures. The thesis can be concluded with some main points as follows:

1. The thesis has successfully fabricated the opto-chemical sensing probe based on FBG by chemical etching (e-FBG) method and high-precision mechanical side-polishing method. In particular, successfully building the measurement configuration of the sensor by integrated the D-FBG sensing probe into the fiber laser configuration with loop-mirror structure has greatly improved the parameters of this sensor. The signal-to-noise ratio (SNR) of the spectral signal is also greatly increased from 3 dB up to 40 dB and the optical signal spectral width of the D - FBG sensor is also greatly reduced from 0.62 nm to 0.01 nm. In addition, the D - FBG sensor integrated into the optical fiber laser with the loop-mirror structure can use saturation pumping technique to

achieve at the intensity of the spectral signal with high power and stable, and then the sensor is only demodulated according to the wavelength shift parameter with high accuracy and can perform well the ability of optical multiplexing to transmit data in long distances.

2. The optical fiber opto-chemical sensor based on eFBG integrated into optical fiber laser configuration with loop-mirror structure is tested for nitrate solutions with concentrations of: 10 ppm, 15 ppm, 30 ppm, 40 ppm, 50 ppm, 60 ppm, 70 ppm and 80 ppm. The result of the sensor is obtained with high sensitivity of S = 0,0035 nm/ppm and limit of detection as LOD = 3 ppm. In which, the safety standard of the World Health Organization (WHO), the nitrate content in clean water is 50 ppm.
3. The D-FBG sensor integrated into the optical fiber laser with loop-mirror structure has been proven feasible through the analysis of organic solvents with refractive index in the range of 1,42 RIU – 1,44 RIU, and achieved a high sensitivity of 33.94 nm/RIU and limit of detection of the sensor as LOD = 2,95 x 10^{-4} RIU.
4. The thesis has successfully fabricated the flat optical fiber SERS substrate with AgNDs nanostructure by assisted-semiconductor laser photochemical method with emission wavelength of 532 nm, and a microsphere optical fiber SERS substrate with AgNDs nanostructures, and AuNPs/AgNDs nanostructures by photochemical using dual-semiconductor laser sources assisted with emission wavelengths 532 nm and 650 nm. The successfully fabricated SERS substrates were

evaluated by Raman spectroscopy method via R6G reagent, the results were obtained with a high surface Raman scattering enhancement coefficient of about 10^7, high stability and uniformity.

5. Based on fabricated optical fiber SERS substrates, we used to detect some samples of substances belonging to the list of pesticides. In which, using the flat fiber optical SERS substrate with AgNDs nanostructure to detect Permethrin and achieved high sensitivity with limit of detection of 0,0035 ppm. The microsphere optical fiber SERS subtrates with AgNDs nanostructure is used to detect Dimethoate, and also achieves high sensitivity and can detect with a concentration as low as 0,05 ppm and limit of detection of 0,001 ppm. The microsphere optical fiber SERS substrates with AuNPs/AgNDs nanostructures were used to analyze samples of Fenthion and Cypermethrin at very low concentrations as ppm and achieved high SERS signal sensitivity and limit of detection of 1,7 x 10^{-4} ppm and 2,87 x 10^{-4} ppm for Fenthion and Cypermethrin, respectively.

The research results obtained in the thesis have proved a great potential for developing high-quality, low-cost photochemical sensors based on optical fiber in the field of testing food safety as well as control of toxic substances exist in the environment.

LIST OF PUBLICATIONS

1. **Thanh Binh Pham**, Thi Hong Cam Hoang, Van Chuc Nguyen, Duc Chinh Vu, Huy Bui, Van Hoi Pham, *"Improved versatile SERS spheroid end-facet optical fiber substrate based on silver nano-dendrites directly planted with gold nanoparticles using dual-laser assisted for pesticides detection"*, Optical Materials, Vol. 126, pp. 112196, 2022.
2. Huy Bui, Thuy Van Nguyen, Thanh Son Pham, Van Hoi Pham, and **Thanh Binh Pham**, "*High enhancement factor of SERS probe based on Silver nano-structures deposited on the silica microsphere by laser-assisted photochemical method"*, Measurement Science and Technology, Vol. 32, pp. 025109, 2021.
3. **Thanh Binh Pham**, Huy Bui, Van Hoi Pham, Thuy Chi Do, *"Surface-enhanced Raman spectroscopy based on Silver nano-dendrites on microsphere end-shape optical fibre for pesticide residue detection",* Optik, Vol. 219, pp. 165172, 2020.
4. **Thanh Binh Pham,** Van Chuc Nguyen, Van Hai Pham, Huy Bui, Roberto Coisson, Van Hoi Pham, and Duc Chinh Vu, "*Fabrication of Silver Nano-Dendrites on Optical Fibre Core by Laser-Induced Method for Surface-Enhanced Raman Scattering Applications"*, Jounal of Nanoscience and Nanotehnology, Vol. 20, no. 3, pp. 1928-1935, 2020.
5. **Thanh Binh Pham**, Thuy Van Nguyen, Thi Hong Cam Hoang, Huy Bui, Thanh Son Pham, Van Phu Nguyen, and Van Hoi Pham, *"Synthesis and deposition of Silver nanostructures on the silica microsphere by a laser-assisted photochemical method for SERS applications"*, Photonics letters of Poland, Vol. 12 (4), pp. 97-99, 2020.
6. **Thanh Binh Pham**, Thi Hong Cam Hoang, Van Hai Pham, Van Chuc Nguyen, Thuy Van Nguyen, Duc Chinh Vu, Van Hoi Pham & Huy Bui, *"Detection of permethrin pesticide using silver nano-dendrites SERS on optical fibre fabricated by laser-assisted photochemical method"*, Scientific Reports, Vol. 9, pp. 12590, 2019.
7. **Pham Thanh Binh**, Nguyen Thuy Van, Pham Van Hoi, Bui Huy, Hoang Thi Hong Cam, Do Thuy Chi, Nguyen Anh Tuan, "*Highly-Sensitivity Refractometer Based on a D-shaped Fiber Bragg Grating Integrated into a Loop-mirror Optical Fiber Laser"*, Communications in Physics, Vol. 32, No. 1, pp. 11-20, 2022.
8. Phạm Văn Hội, Bùi Huy, **Phạm Thanh Bình**, Nguyễn Thúy Vân, "*Đầu dò cảm biến sử dụng cách tử Bragg trong sợi quang ăn mòn một phần (e-FBG) có phủ lớp chức năng để nâng cao độ chọn lọc tác nhân đo và sử dụng được nhiều lần*", Bằng sáng chế Việt Nam số: 1-0028193, 2021.
9. Phạm Văn Hội, **Phạm Thanh Bình**, Bùi Huy, Hoàng Thị Hồng Cẩm, Nguyễn Thúy Vân, Phạm Thanh Sơn, "*Cảm biến quang tử tăng cường tán xạ Raman bề mặt (SERS) sử dụng vi cầu thủy tinh silica phủ lớp nano bạc cấu trúc cành lá chế tạo bằng phương pháp quang hóa trợ giúp bằng laze"*, Bằng sáng chế Việt Nam số: 1-0032301, 2022.
10. **Phạm Thanh Bình**, Nguyễn Văn Ấn, Nguyễn Thúy Vân, Hoàng Thị Hồng Cẩm, Dương Thị Hường, Phạm Nam Thắng, Vũ Đức Chính, Đỗ Thùy Chi, Bùi Huy và Phạm Văn Hội, *"Chế tạo đế SERS vi thấu kính quang sợi với nano Au/Ag dạng cành lá để phân tích chất bảo vệ thực vật",* Tuyển tập báo cáo của Hội nghị vật lý chất rắn và khoa học vật liệu toàn quốc lần thứ 12 (SPMS 2021), pp. 713-718, 2022.
11. **T. B. Pham**, H. T. Le, H. Bui, and V. H. Pham, *"Characteristics of the fiber laser sensor system based on etched-Bragg grating sensing probe for determination of the low nitrate concentration in water",* Sensors, Vol. 17(1), pp. 7, 2017.
12. **Phạm Thanh Bình**, Phạm Văn Hội, Bùi Huy, Lê Hữu Thắng, Nguyễn Đức Bình, Phạm Văn Đại, *"Đầu dò cảm biến cách tử Bragg trong sợi quang (E-FBG) và phương pháp chế tạo",* Bằng sáng chế Việt Nam số: 20409, 2019.